Aquatic Toxicology 225 (2020) 105541

Contents lists available at ScienceDirect

Aquatic Toxicology

journal homepage: www.elsevier.com/locate/aqtox

Combined effects of nano-TiO_2 and hexavalent chromium towards marine crustacean *Artemia salina*

Vignesh Thiagarajan[a], R. Seenivasan[a], David Jenkins[b], N. Chandrasekaran[a], Amitava Mukherjee[a,*]

[a] Centre for Nanobiotechnology, Vellore Institute of Technology (VIT), Vellore 632014, India
[b] Wolfson Nanomaterials & Devices Laboratory, School of Computing, Electronics and Mathematics, Faculty of Science & Engineering, University of Plymouth, Devon, PL4 8AA, UK

ARTICLE INFO

Keywords:
Agglomeration
Artemia salina
Cr(VI)
Nano-TiO_2
Toxicity

ABSTRACT

There has been a significant increased concern of the impact of the toxicity of multiple contaminants in the marine environment. Thus, this study was aimed at determining whether the interaction between nano-TiO_2 and Cr(VI) would modulate their toxic effects with the marine crustacean, *Artemia salina*. Nano-TiO_2 agglomerated in artificial sea water (ASW) and readily formed micron-sized particles that settled down in the medium. The addition of Cr(VI) to nano-TiO_2 aggravated their agglomeration through sorption of Cr(VI) onto nano-TiO_2. This was reflected by a decrease in the residual concentration of Cr in the suspension. Acute toxicity tests performed using pristine nano-TiO_2 (0.25, 0.5, 1, 2, and 4 mg/L) and Cr(VI) (0.125, 0.25, 0.5, and 1 mg/L) displayed a concentration dependent rise in the mortality of *Artemia salina*. To examine the effects of mixtures of nano-TiO_2 and Cr(VI) on *Artemia salina*, two groups of experiments were designed. The former group studied the toxic effect of nano-TiO_2 (0.5, 1, 2, and 4 mg/L) with a fixed concentration (0.125 mg/L) of Cr(VI). While the latter group studied the toxicity of Cr(VI) (0.25, 0.5, and 1 mg/L) with a fixed concentration (0.25 mg/L) of nano-TiO_2. The toxic effects of nano-TiO_2 was not significantly reduced at a fixed concentration of Cr(VI) but in contrast, a significant reduction in the Cr(VI) toxicity by fixed concentration of nano-TiO_2 was observed. Toxicity data was well supported by an independent action model that proved the mode of action between nano-TiO_2 and Cr(VI) to be antagonistic. Furthermore, ROS generation and measurement of antioxidant enzyme activities were also in line with toxicity results. From this study, the modification of Cr(VI) toxicity at fixed concentration of nano-TiO_2 could have a huge impact on the reduction in Cr(VI) toxicity across trophic levels.

1. Introduction

Among various metal oxide nanomaterials, titanium dioxide nanoparticles (nano-TiO_2) has been a part of our daily lives. They are extensively used in day-to-day commodities such as cosmetics, paints, skin care products etc. (Gupta et al., 2019). Attributed to its increased large-scale production, nano-TiO_2 has become one of the emerging contaminant of the marine environment. Their entry into the marine environment could either be deliberate or accidental and happens through surface run-off, household, industrial and hospital waste discharges (Fazelian et al., 2019). With these discharges, the expected concentration of nano-TiO_2 in aquatic environments will soon reach micrograms per litre levels (Doyle et al., 2015). Even such low concentrations of nano-TiO_2 pose a major threat to marine species, and hence an imperative assessment of their toxic impacts needs to be immediately addressed.

Likewise, environmental contamination by heavy metals also presents a major ecological factor and an associated health risk. Chromium [Cr] was chosen as the heavy metal to focus on in this study as it has been listed by the Environmental Protection Agency as one of the most common and noxious contaminants (Sharma et al., 2012; Vimercati et al., 2017) and has been used as a soluble reference chemical for toxicity testing in *Artemia salina* (Kos et al., 2016; Persoone et al., 1989). Cr primarily exist in two stable oxidation states: hexavalent Cr [Cr(VI)] and trivalent Cr [Cr(III)]. Cr(VI) is highly toxic, stable and soluble in sea water (Bonnand et al., 2013) compared to Cr(III). Entry into seawater occurs either through natural [leaching from top soil and rocks] or anthropogenic sources [industrial establishments] (Oze et al., 2007; Tchounwou et al., 2012). Although their concentration in seawater remains very low [5.2×10^{-6} mg/L – 832×10^{-6} mg/L], their

* Corresponding author.
E-mail addresses: amitav@vit.ac.in, amit.mookerjea@gmail.com (A. Mukherjee).

https://doi.org/10.1016/j.aquatox.2020.105541
Received 3 May 2020; Received in revised form 3 June 2020; Accepted 6 June 2020
Available online 12 June 2020
0166-445X/

toxic impact cannot simply be overlooked (Pađan et al., 2019). The determination of toxicity produced from such low concentrations of Cr (VI), along with a co-contaminant, such as nano-TiO_2 to marine organism is essential.

It has been shown that multiple contaminants can co-exist in the marine environment and that they may work together to either enhance or subdue their toxicity to marine organisms (Heys et al., 2016). In this regard, nano-TiO_2 and Cr(VI) was chosen as the model contaminant to mimic the environmental conditions and evaluate how they influence their toxicity over one another. Although several studies dealt with mixture effects of nano-TiO_2 and heavy metals on freshwater organisms (Hu et al., 2019; Li et al., 2017, 2016; Luo et al., 2018), there are limited studies on their effects on marine organisms. Balbi et al. (2014) reported no alteration in the bioavailability, bioconcentration and toxicity profile of Cd^{2+} upon co-exposure with nano-TiO_2 to the marine bivalve *Mytilus galloprovincialis*. In particular, no study had previously dealt with evaluating the toxic effects of nano-TiO_2 in combination with Cr(VI). Therefore, filling this knowledge gap is very crucial.

Ecotoxicological analysis have been used to monitor the environmental impact of the contaminants in the marine environment. Bioindicators play a critical role in carrying out such analysis as they are sensitive to very low concentrations of contaminants, and respond well to environmental stress (Parmar et al., 2016). In the marine environment, zooplankton forms a major depository of organisms that help in channelling the flow of energy across the food chain (Ozkan et al., 2016). Amongst various zooplanktons, *Artemia salina* was chosen as the test organism because of their non-selective filter feeding behaviour and high reproductive capacity (Ates et al., 2016; Gutner-Hoch et al., 2019).

Considering the lack of published literature, the present study is the first of its kind to report the toxic effects of this mixture of nano-TiO_2 and Cr(VI) on marine organisms. We hereby hypothesize that a possible interaction between Cr(VI) and nano-TiO_2 might influence their toxic effects *to Artemia salina*. The major purpose of this study was to evaluate; (i) the impact of Cr(VI) on nano-TiO_2 toxicity and (ii) the effects of nano-TiO_2 on Cr(VI) toxicity. Initially, nano-TiO_2, with and without Cr (VI), were characterised using electron microscopy and particle size analysis. Two groups of mixture concentrations were then created to examine their toxic impacts on *Artemia salina*. The first group consisted of varying nano-TiO_2 (0.5, 1, 2, and 4 mg/L) with a fixed concentration (0.125 mg/L) of Cr(VI), while the second group consisted of varying Cr (VI) (0.25, 0.5, and 1 mg/L) with a fixed concentration (0.25 mg/L) of nano-TiO_2. The toxicity profile was further validated by the subsequent changes in oxidative radical generation, antioxidant enzyme activity and morphological traits in the organism.

2. Materials and methods

2.1. Chemicals

For this work, P25, a form of nano-TiO_2 powder having a primary particle size of 21 nm, 2′, 7′ dichlorofluorescin diacetate (DCFH-DA) and sodium carbonate (Na_2CO_3) were bought from Sigma-Aldrich, USA. Hydroxylamine hydrochloride, dimethyl sulfoxide, and Triton X-100 were sourced from Hi-Media Pvt. Ltd., India. Potassium dichromate ($K_2Cr_2O_7$) was obtained from SRL Chemicals Pvt. Ltd., India. Nitroblue tetrazolium chloride (NBT) and 30 % w/v Hydrogen peroxide (H_2O_2) were purchased from SDFCL, India. The eggs of *Artemia salina* were purchased from Ocean Star International Inc., USA.

2.2. Preparation of stock dispersions of nano-TiO_2 and Cr(VI)

P25 form of nano-TiO_2 was added to deionized water to prepare an initial stock dispersion of 100 mg/L. The prepared suspension was sonicated for 30 min using a probe sonicator to obtain a uniform dispersion. For the preparation of the stock solution of 1000 mg/L Cr(VI), 28.35 mg of $K_2Cr_2O_7$ was dissolved in 10 mL of deionized water.

2.3. Experimental matrix and test organism

Natural seawater (NSW) was used to hatch *Artemia salina* eggs, whereas artificial seawater (ASW) (Supplementary information) was used as the experimental matrix for performing toxicity and biochemical assays. Both seawater types were filtered and sterilized at 121 ˚C for 20 min. About 1 g of dried eggs were added to 2 L of NSW in a round bottom glass tank, with a constant supply of air and light provided. Under these conditions, hatching occurred within a day and the hatched nauplii were separated and allowed to grow in a fresh NSW medium for a further 24 h. For the experiments, 48-h old nauplii were selected. All assays in this study were conducted using an established protocol (Bhuvaneshwari et al., 2018).

2.4. Assessment of physical-chemical interactions between nano-TiO_2 and Cr(VI)

Nano-TiO_2 dispersed in deionized water was characterized for shape and size using high resolution transmission electron microscope (TEM) (FEI TecnaiG2 T20 S-twin). Also, the behaviour of nano-TiO_2, with and without Cr(VI) in ASW was also assessed using TEM. Nano-TiO_2 concentration of 0.25 mg/L with and without 1 mg/L Cr(VI) and nano-TiO_2 concentration of 4 mg/L with and without 0.125 mg/L Cr(VI) were prepared and a selection of samples were dropped onto a copper grid and imaged using TEM.

To assess the effective diameter of nano-TiO_2, 0.25 mg/L nano-TiO_2 with and without 1 mg/L Cr(VI), and 4 mg/L nano-TiO_2 with and without 0.125 mg/L Cr(VI), were prepared in ASW and analysed immediately using a particle size analyser (Brookhaven Instruments Corp., USA). To carry out the sedimentation analysis, a selection of samples from these dispersions were pipetted out from the top portion of the static suspension and the absorbance maximum of nano-TiO_2 was recorded (324 nm) (Model U2910, HITACHI, Japan).

2.5. Determination of residual concentration of Cr

The residual concentration of Cr was determined at different time points for the mixtures containing 1 mg/L Cr(VI) with a fixed concentration of nano-TiO_2 (0.25 mg/L) and 4 mg/L nano-TiO_2 with a fixed concentration of Cr(VI) (0.125 mg/L). After the stipulated time points (0, 24, and 48 h), samples were centrifuged (12,000 rpm, 15 min) and the supernatant was filtered using 0.1 μm and 3 KDa filters for the complete elimination of nano-TiO_2. The filtered supernatant was analysed for Cr concentration at a wavelength of 357.87 nm with an Atomic Absorption Spectrophotometer (Perkin Elmer, India).

2.6. Determination of acute toxicity

2.6.1. Determination of toxic effects of pristine nano-TiO_2 and Cr(VI)

The test concentrations for toxicity test were selected based on the EC_{50} values of pristine nano-TiO_2 (2 mg/L) and Cr(VI) (0.3 mg/L). For nano-TiO_2, three concentrations < EC_{50} value (0.25, 0.5, and 1 mg/L), one concentration nearer to EC_{50} value (2 mg/L), and one > EC_{50} value (4 mg/L) were chosen. Similarly, for Cr(VI), two concentrations < EC_{50} value (0.125, and 0.25 mg/L), one concentration nearer to EC_{50} value (0.5 mg/L), and one > EC_{50} value (1 mg/L) were chosen. Thus, acute toxicity experiments were conducted with five varying concentrations of pristine nano-TiO_2 (0.25, 0.5, 1, 2, and 4 mg/L) and four varying concentrations of Cr(VI) (0.125, 0.25, 0.5, and 1 mg/L). All toxicity and biochemical tests were performed in triplicates. Around 10 *Artemia salina* nauplii were interacted with the above-mentioned concentrations of pristine nano-TiO_2 and Cr(VI), and after an exposure period of 48 h, the total live nauplii were counted and the percentage of mortality was calculated, keeping control samples as a reference. No aeration or food

was provided to nauplii during the experiments.

2.6.2. Determination of mixture toxicity of nano-TiO_2 and Cr(VI)

Two groups of experiments were created for assessing the toxicity of nano-TiO_2 and Cr(VI) mixtures. The former group studied how Cr(VI) modulates the toxicity of nano-TiO_2, while the latter group studied how nano-TiO_2 influences the toxicity of Cr(VI). The former group experiments were carried out with varying concentrations of nano-TiO_2 (0.5, 1, 2, and 4 mg/L) and fixed Cr(VI) of 0.125 mg/L. Similarly the second group of experiments consisted of varying concentrations of Cr(VI) (0.25, 0.5, and 1 mg/L) and fixed nano-TiO_2 of 0.25 mg/L. Around 10 *Artemia salina* nauplii were used for interaction and after an exposure period of 48 h, the total live nauplii were counted and percentage of mortality was calculated, keeping control samples as a reference. No food and aeration were provided to nauplii during the experiments.

The toxicity results were further substantiated by an independent action model. This model is used when the mode of action of two contaminants under study is different (Abbott, 1925). Expected mortality (C_{exp}), and inhibition ratio (R_I) were computed on the basis of the equations provided in our previous publication (Thiagarajan et al., 2019). The R_I value determines the mode of interaction between nano-TiO_2 and Cr(VI). An R_I value <1 indicates an antagonistic action while R_I value >1 shows a synergistic action. Whereas $R_I = 1$ indicates an additive mode of interaction. Two-way ANOVA was performed to check the significance between observed and expected mortality. If no significance exists between observed and expected mortality, the interaction is additive, irrespective of the acquired R_I value.

2.7. Determination of oxidative stress

2.7.1. Estimation of reactive oxygen species (ROS)

ROS are generated in response to the stress generated by contaminants in the system and was quantified by the procedure described previously (Wang and Joseph, 1999). After the treatment of *Artemia salina* with pristine nano-TiO_2, Cr(VI), and mixture groups, the nauplii were rinsed in deionized water. About 100 µL of DCFH-DA (10 µM) was added and incubated in the dark for 30 min. Afterwards, the nauplii were rinsed in deionized water and 2 mL of phosphate buffer (pH 7.4) was added and homogenized. The homogenized samples were centrifuged, and the supernatant was analysed for fluorescent intensity at an excitation wavelength of 485 nm, with an emission wavelength of 530 nm (Cary Eclipse fluorescence spectrophotometer, model G9800A; Agilent Technologies, USA).

2.7.2. Estimation of antioxidant enzyme activity

Artemia salina treated with pristine nano-TiO_2, Cr(VI), and mixture groups were rinsed in deionized water. After rinsing, the nauplii were homogenized in a 0.5 M potassium phosphate buffer of pH 7.5. Afterwards, centrifugation of the samples was carried out for 10 min at 13,000 rpm and the recovered supernatant was used to perform the following bioassays.

Quantification of SOD activity is essential in the antioxidant properties of a biological system and this was performed using the characterizing protocol explained by Kono (1978). The assay was performed in a 24 well plate by the addition of the following reagents, one after the other: 50 mM of Na_2CO_3 buffer (pH 10), 96 of mM NBT, 0.6 % of Triton X-100, 20 mM of hydroxylamine hydrochloride, and 70 µL of the recovered supernatant. The prepared reaction mixture was placed under visible illumination (fixed wavelength) for 20 min and absorbance of the reaction mixture was recorded at 560 nm using an UV–vis spectrophotometer.

The CAT activity in response to oxidative stress was estimated (Yilancioglu et al., 2014). 200 µL of the recovered supernatant was added to 10.8 mM H_2O_2 prepared in 50 mM potassium phosphate buffer and this reaction mixture was measured spectrophotometrically at 240 nm for 3 min using an UV–vis spectrophotometer. Potassium phosphate buffer was used as the reference.

2.8. Optical microscopy

In order to assess the morphological damage, optical microscopic images were captured for the control nauplii, and the nauplii treated with 4 mg/L pristine nano-TiO_2, 1 mg/L Cr(VI), 4 mg/L nano-TiO_2 with fixed Cr(VI) of 0.125 mg/L, and 1 mg/L Cr(VI) with fixed nano-TiO_2 of 0.25 mg/L. The nauplii was placed on the glass slide, fixed with 2 % glutaraldehyde and imaged under a phase contrast microscope (Zeiss Axiostar Optical Microscope, USA).

2.9. Statistical analysis

All tests were conducted in triplicates ($n = 3$) and the findings were recorded as mean ± standard error. To test the statistical significance of the data, two-way ANOVA with a Bonferroni post-test was carried out and the statistical significance was set at $p < 0.05$.

3. Results

3.1. Physical-chemical interactions

Fig. 1 shows spherical and cubic shaped nano-TiO_2 particles with a size less than 25 nm. The agglomeration of nano-TiO_2 in ASW (0^{th} h) with and without Cr(VI) is depicted in Fig. 2. It was observed that 4 mg/L nano-TiO_2 (Fig. 2A) showed more agglomeration compared to 0.25 mg/L nano-TiO_2 (Fig. 2B). This agglomeration of nano-TiO_2 marginally increased in the presence of Cr(VI) (Fig. 2C and D).

The agglomeration was further validated from dynamic light scattering studies. The effective diameter of nano-TiO_2 in ASW with and without Cr(VI) at different time intervals is depicted in Fig. 3A. A dose-dependent increase in the size of NPs over time was observed with and without Cr(VI). This increase in the effective diameter of nano-TiO_2 upon Cr(VI) addition (4 mg/L nano-TiO_2 with 0.125 mg/L Cr(VI) and 1 mg/L Cr(VI) with 0.25 mg/L nano-TiO_2) was significant ($p < 0.05$) with respect to the effective diameter of pristine nano-TiO_2 (4 mg/L and 0.25 mg/L).

Sedimentation of nano-TiO_2 in ASW also validated their agglomeration in the test medium (Fig. 3B). A decrease in the absorbance of nano-TiO_2 from the top layer of the static suspension was observed for

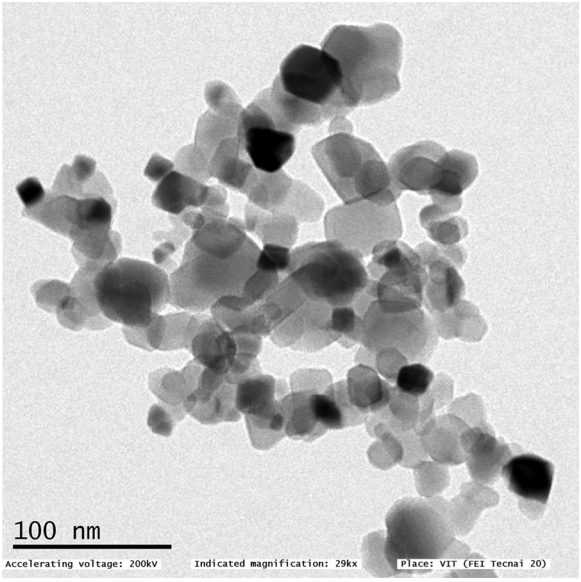

Fig. 1. Transmission electron microscopic image of nano-TiO_2 dispersion in deionized water.

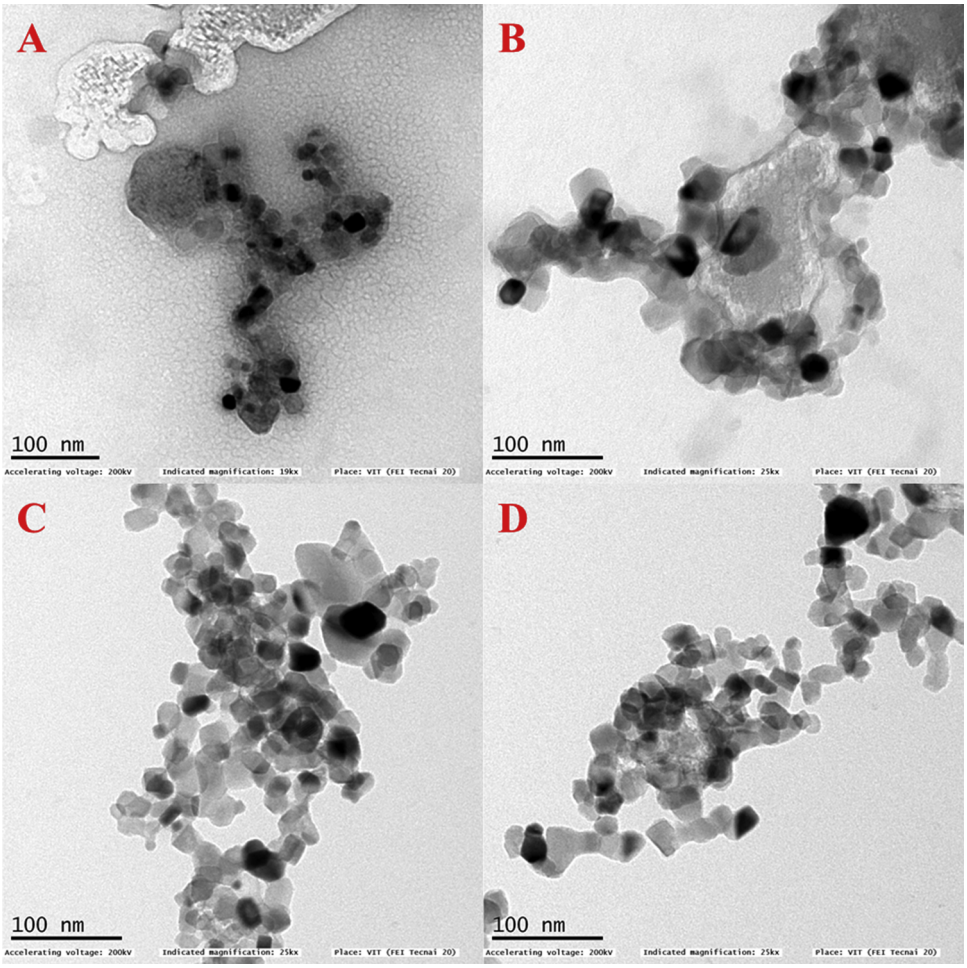

Fig. 2. Transmission electron microscopic image of A) 4 mg/L nano-TiO_2; B) 0.25 mg/L nano-TiO_2; C) 4 mg/L nano-TiO_2 + 0.125 mg/L Cr(VI); D) 1 mg/L Cr(VI) + 0.25 mg/L nano-TiO_2 in the experimental matrix (ASW).

both mixture groups. After 48 h, about 5.7 % of 4 mg/L pristine nano-TiO_2, and 16.6 % of 0.25 mg/L pristine nano-TiO_2 were available in the top portion indicating the settling of NPs in the system. While in the presence of 0.125 mg/L Cr(VI), about 7.5 % of 4 mg/L nano-TiO_2 was available. The decrease in the settling percentage was statistically insignificant for 4 mg/L nano-TiO_2 with and without 0.125 mg/L Cr(VI). However, no absorbance peak of nano-TiO_2 was obtained when 1 mg/L Cr(VI) was added to it.

3.2. Cr (VI) adsorption on nano-TiO_2

Determination of the residual concentration of Cr is a measure of Cr(VI) adsorption over nano-TiO_2. At 0^{th} h, for the mixture containing 4 mg/L nano-TiO_2 and 0.125 mg/L Cr(VI), the percentage of Cr adsorbed over nano-TiO_2 was found to be 23 ± 8 %, which increased to 48 ± 2 % after 48 h. But in contrast, for the mixture containing 1 mg/L Cr(VI) and 0.25 mg/L nano-TiO_2, the percentage of Cr adsorbed over nano-TiO_2 at 0^{th} h was found to be 33 ± 4 % and reached an equilibrium value of 21 ± 1 % after 48 h.

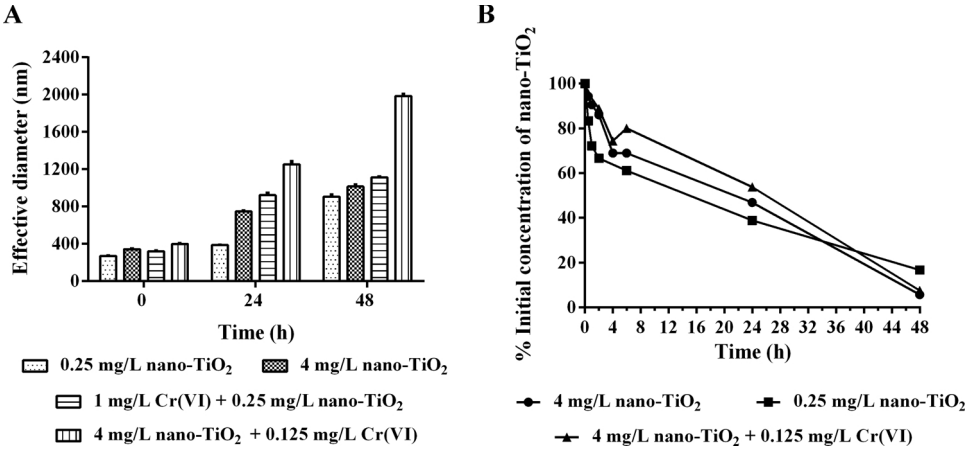

Fig. 3. A) Effective diameter of nano-TiO_2 nanoparticles in ASW, and B) Sedimentation profile of nano-TiO_2 with and without Cr(VI).

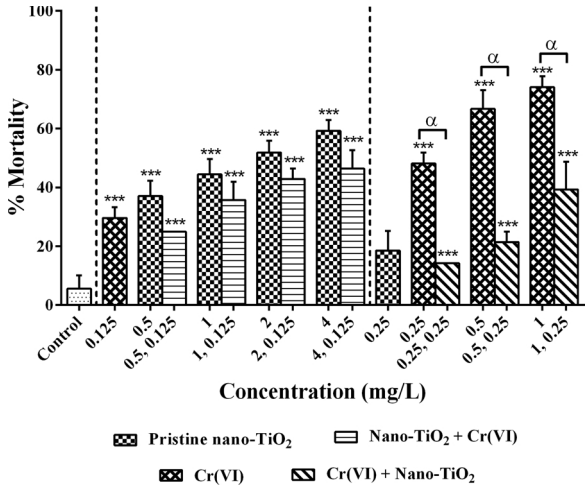

Fig. 4. Percentage mortality produced in response to pristine nano-TiO_2 (0.25, 0.5, 1, 2, and 4 mg/L), Cr(VI) (0.125, 0.25, 0.5, and 1 mg/L) and their mixture. '*' indicates significant difference in mortality with respect to control whereas 'α' represents significant difference in mortality between mixture concentration and respective concentrations of pristine nano-TiO_2/Cr(VI).

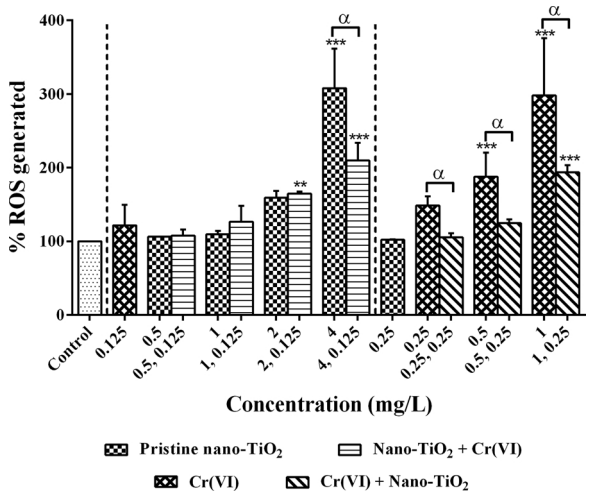

Fig. 5. Percentage ROS produced in response to pristine nano-TiO_2 (0.25, 0.5, 1, 2, and 4 mg/L), Cr(VI) (0.125, 0.25, 0.5, and 1 mg/L) and their mixture. '*' indicates significant difference in ROS generation with respect to control whereas 'α' represents significant difference in ROS generation between mixture concentration and respective concentrations of pristine nano-TiO_2/Cr(VI).

3.3. Mixture effect of nano-TiO_2 and Cr(VI)

The mortality observed in response to the treatment of pristine nano-TiO_2 and Cr(VI) on *Artemia salina* is depicted in Fig. 4. This interaction, with increasing concentrations of pristine nano-TiO_2 and Cr (VI), resulted in an increase in mortality, which was significantly different ($p < 0.001$) from the control, except for 0.25 mg/L of pristine nano-TiO_2.

The mortality observed in response to the treatment of the mixture groups on *Artemia salina* is also depicted in Fig. 4. A concentration dependent rise in mortality was observed after the addition of 0.125 mg/L Cr(VI) to increasing concentrations of nano-TiO_2 (0.5, 1, 2, and 4 mg/L). This rise in mortality was significantly different ($p < 0.001$) from the control. Similar significant increase ($p < 0.001$) in the mortality was documented after the addition of 0.25 mg/L nano-TiO_2 to different concentrations of Cr(VI) (0.25, 0.5, and 1 mg/L).

The addition of 0.125 mg/L Cr(VI) reduced the toxicity of nano-TiO_2 for *Artemia salina* when compared with their respective pristine nano-TiO_2 concentrations. The observed decline between pristine nano-TiO_2 and nano-TiO_2 + Cr(VI) was statistically insignificant ($p > 0.05$) for all the test concentrations. Likewise, the addition of 0.25 mg/L nano-TiO_2 reduced the toxicity of Cr(VI) to *Artemia salina* when compared with respective pristine Cr(VI) concentrations. However, this decline observed between pristine Cr(VI) and Cr(VI) + nano-TiO_2 was highly significant ($p < 0.001$) at all test concentrations.

The mixture toxicity of nano-TiO_2 and Cr(VI) was substantiated by an independent action model. Table 1 shows the calculated R_I value along with their respective mode of action between the contaminants. A concentration dependent increase in the R_I values were noted upon the addition of 0.125 mg/L Cr(VI) with increasing concentrations of nano-TiO_2 (0.5, 1, 2, and 4 mg/L). Similarly, an increasing trend in the R_I values were observed after the addition of 0.25 mg/L nano-TiO_2 to different concentrations of Cr(VI) (0.25, 0.5, and 1 mg/L). As the R_I values are <1 and a significant difference ($p < 0.05$) exists between the observed and expected mortality, the mode of action between nano-TiO_2 and Cr(VI) in both the mixture groups were antagonistic. Thus, this model validates the results of the toxicity profile.

3.4. Oxidative stress

3.4.1. Reactive oxygen species

The production of ROS in *Artemia salina* after treatment with pristine nano-TiO_2 and Cr(VI) is shown in Fig. 5. The interaction with increasing concentrations of pristine nano-TiO_2 and Cr(VI) resulted in an increase in ROS production, which was statistically different ($p < 0.001$) from the control only for 4 mg/L of pristine nano-TiO_2 and 0.5, and 1 mg/L of Cr(VI).

ROS produced in *Artemia salina* after treatment with mixture groups is also depicted in Fig. 5. A concentration dependent rise in ROS generation was recorded after the addition of 0.125 mg/L Cr(VI) to varying concentrations of nano-TiO_2 (0.5, 1, 2, and 4 mg/L) and for the addition of 0.25 mg/L nano-TiO_2 to varying concentrations of Cr(VI) (0.25, 0.5, and 1 mg/L). This increased ROS generation was significantly different ($p < 0.001$) from control only for two mixture concentrations: 4 mg/L nano-TiO_2 + 0.125 mg/L Cr(VI) and 1 mg/L Cr(VI) + 0.25 mg/L nano-TiO_2.

The addition of 0.125 mg/L Cr(VI) to 4 mg/L nano-TiO_2 resulted in a significant decrease ($p < 0.05$) in ROS generation when compared with 4 mg/L pristine nano-TiO_2 alone. In contrast, the addition of 0.25 mg/L nano-TiO_2 to varying concentrations of Cr(VI) (0.25, 0.5, and 1

Table 1
Independent action model for the mixture containing nano-TiO2 and Cr(VI).

Concentration of Cr(VI) (mg/L)	Concentration of nano-TiO_2 (mg/L)	Observed Toxicity (%)	Expected Toxicity (%)	Ratio of Inhibition (R_I)	$p<0.05$	Mode of action
0.125	0.5	25	51.99 ± 4.61	0.48 ± 0.04	Yes	**Antagonistic**
	1	35.71 ± 6.18	57.77 ± 5.12	0.64 ± 0.14	Yes	**Antagonistic**
	2	42.85 ± 3.57	63.55 ± 2.35	0.67 ± 0.04	Yes	**Antagonistic**
	4	46.42 ± 6.18	68.88 ± 3.87	0.68 ± 0.12	Yes	**Antagonistic**
0.25	0.25	14.28 ± 0.00	54.66 ± 1.33	0.26 ± 0.00	Yes	**Antagonistic**
0.5		21.42 ± 3.57	70.66 ± 5.55	0.30 ± 0.04	Yes	**Antagonistic**
1		39.28 ± 9.44	76.88 ± 4.44	0.50 ± 0.10	Yes	**Antagonistic**

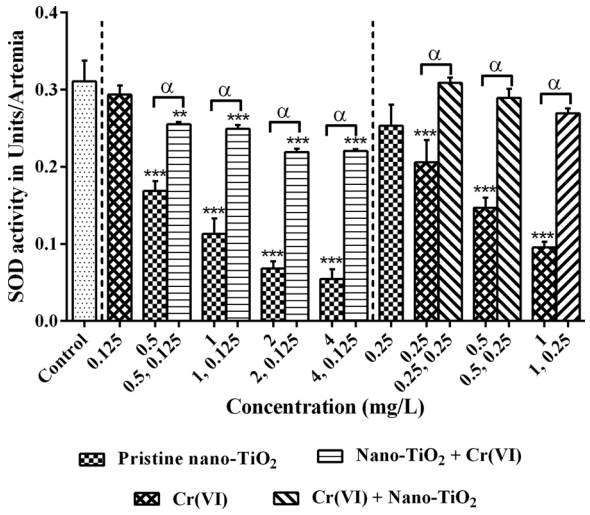

Fig. 6. SOD activity produced in response to pristine nano-TiO_2 (0.25, 0.5, 1, 2, and 4 mg/L), Cr(VI) (0.125, 0.25, 0.5, and 1 mg/L) and their mixture. '*' indicates significant difference in SOD activity with respect to control whereas 'α' represents significant difference in SOD activity between mixture concentration and respective concentrations of pristine nano-TiO_2/Cr(VI).

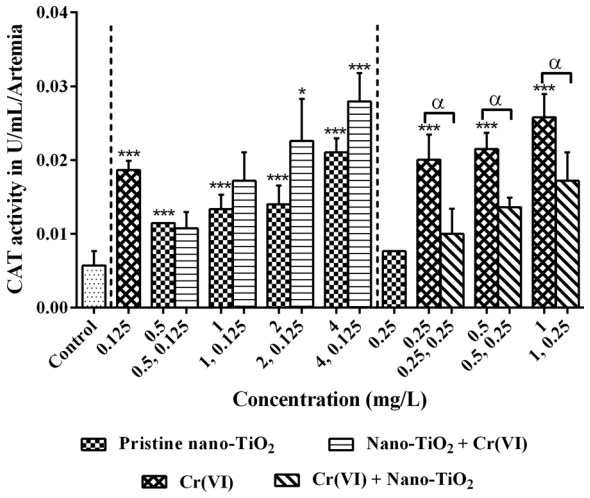

Fig. 7. CAT activity produced in response to pristine nano-TiO_2 (0.25, 0.5, 1, 2, and 4 mg/L), Cr(VI) (0.125, 0.25, 0.5, and 1 mg/L) and their mixture. '*' indicates significant difference in CAT activity with respect to control whereas 'α' represents significant difference in CAT activity between mixture concentration and respective concentrations of pristine nano-TiO_2/Cr(VI).

mg/L) produced a significant decrease ($p < 0.05$) in ROS generation for all the mixture concentrations when compared with respective pristine Cr(VI) concentrations.

3.4.2. Antioxidant enzyme activity

SOD activity in *Artemia salina* after treatment with pristine nano-TiO_2, Cr(VI), and their mixtures is represented in Fig. 6. Their interaction with increasing concentrations of pristine nano-TiO_2 and Cr(VI) resulted in reduced SOD activity, which was statistically different ($p < 0.001$) from the control, except for 0.25 mg/L of pristine nano-TiO_2. Similarly, for the first mixture group, a concentration dependent significant reduction ($p < 0.01$) in SOD activity with control was recorded after the addition of 0.125 mg/L of Cr(VI) to varying concentrations of nano-TiO_2 (0.5, 1, 2, and 4 mg/L). Whereas for the second mixture group, the addition of 0.25 mg/L nano-TiO_2 to varying concentrations of Cr(VI) (0.25, 0.5, and 1 mg/L) produced an insignificant reduction ($p > 0.05$) in SOD activity with respect to the control. When comparing pristine nano-TiO_2 with nano-TiO_2 + Cr(VI) and pristine Cr(VI) with Cr(VI) + nano-TiO_2, a statistically significant ($p < 0.001$) increase in the SOD activity was recorded.

CAT activity in *Artemia salina* after treatment with pristine nano-TiO_2, Cr(VI), and their mixture is depicted in Fig. 7. Increasing concentrations of pristine nano-TiO_2 and Cr(VI) resulted in increased CAT activity, which was statistically different ($p < 0.001$) from the control, except for 0.25 mg/L of pristine nano-TiO_2. Similarly, the addition of 0.125 mg/L Cr(VI) to 2 and 4 mg/L of nano-TiO_2 produced a significant increase in CAT activity ($p < 0.05$) with respect to the control. In contrast, the addition of 0.25 mg/L nano-TiO_2 to varying concentrations of Cr(VI) (0.25, 0.5, and 1 mg/L) produced an insignificant increase ($p > 0.05$) in CAT activity with respect to the control for all the mixture concentrations. Comparisons between pristine nano-TiO_2 and nano-TiO_2 + Cr(VI) showed an insignificant ($p > 0.05$) increase in CAT activity, whereas comparisons between pristine Cr(VI) and Cr(VI) + nano-TiO_2 showed a highly significant reduction ($p < 0.001$) in CAT activity for all the test concentrations.

3.5. Morphological changes

The morphological damage to *Artemia salina* treated with nano-TiO_2, Cr(VI), and their mixture were represented in Fig. S1. No noticeable damage or particle intake was observed in the nauplii control group (Fig. S1A). Nauplii treated with pristine nano-TiO_2 (4 mg/L) had ingested and accumulated NPs from the thorax to the last appendages of the abdominal gut region, with minimal physical deformities observed (Fig. S1B). For the nauplii treated with 1 mg/L Cr(VI), the following observations were recorded: both antennules were missing, clear stooping of the abdominal region, mislaid and distortion of both antenna, protuberance and narrowed whole body length (Fig. S1C). Small agglomerates of Cr(VI) adsorbed on *Artemia* might hinder its typical swimming patterns. Nauplii treated with mixture groups demonstrated abysmal physical deformities such as missing an eye and both the antennule and antenna (Fig. S1D and S1E). Agglomerates of nano-TiO_2 and Cr(VI) were evenly adsorbed on the body surface (Fig. S1E) and its ingestion was evident by its presence in the abdominal region (gut). Swelling of the whole body, complete damage to the thoracic region and a slouching abdominal gut were also evident.

4. Discussion

The highly saline nature of seawater reduces the electrostatic repulsion between the particles, which results in agglomeration of nano-TiO_2 (Manzo et al., 2015). Thus formed micron and submicron-sized agglomerates are also capable of producing toxic effects (Schiavo et al., 2018). The addition of Cr(VI) to nano-TiO_2 further accelerated the agglomeration (Fig. 3A). At a slightly alkaline pH > 8, Cr(VI) could exist as CrO_4^{2-} (Weng et al., 1997), which might facilitate the anionic adsorption onto nano-TiO_2 (Yang and Lee, 2006). In addition, nano-TiO_2 has relatively a high adsorption potential for Cr(VI) due to the presence of hydroxyl group (OH) on the surface (Asuha et al., 2010). Further studies related to surface chemical changes of nano-TiO_2 are required to understand this enhanced agglomeration phenomenon. This agglomeration could not significantly affect the bioavailable nano-TiO_2 concentration (Fig. 3B), since even at the highest nano-TiO_2 concentration (4 mg/L), only 0.062 mg/L Cr(VI) was adsorbed (Section 3.2). When the adsorption equilibrium is reached, an instantaneous desorption of Cr(VI) may follow, thereby reducing the further surface binding of Cr(VI) on nano-TiO_2. Our observations are similar to the findings of Weng et al. (1997) and Yang and Lee (2006).

Because of significant agglomeration and sedimentation in the medium, the concentration of nano-TiO_2 was not linearly associated to the initial amount of nano-TiO_2 (Brunelli et al., 2013). Hence, the mortality of *Artemia salina* would be mainly dependent on initial uptake of nano-TiO_2. In the binary mixture, almost 50 % nano-TiO_2 (24 h)

(Fig. 3B) was available either in free or complex (nano-TiO_2–Cr(VI)) form in the medium, and this could have induced toxicity in *Artemia salina*. Furthermore, higher concentrations of nano-TiO_2 could efficiently adsorb Cr(VI), thereby decreasing Cr(VI) availability and attenuating its toxicity. It is also observed that addition of 0.25 mg/L nano-TiO_2 to different concentrations of Cr(VI) significantly reduced the toxic effects of Cr(VI). As the cut-off size for particle ingestion by *Artemia salina* is 50 μm (Ates et al., 2013), even micron sized nano-TiO_2 with adsorbed Cr(VI) could enter and accumulate in the acidic gut regions (Fig. S1). The desorption of Cr(VI) from nano-TiO_2 at such a low pH would be rather difficult. (Lu et al., 2018). Additionally, acidic pH conditions would also favour photocatalytic conversion of Cr(VI) to Cr (III) on the surface of nano-TiO_2, thereby reducing the toxic impact of adsorbed Cr (Marinho et al., 2017; Wang et al., 2004).

From the mortality data, it is obvious that the toxicity induced by both the mixture groups were antagonistic and this was validated from independent action modelling (Table 1). The presence of nano-TiO_2 with Cr(VI) could prevent the synergy of the mixture compounds by the adsorption of Cr(VI) on nano-TiO_2, thereby producing an antagonistic effect to *Artemia salina* (Matouke and Mustapha, 2019). This result was well supported with the findings of Li et al. (2018) where the toxicity produced by the mixture containing nano-TiO_2 and Cd^{2+} was antagonistic to *Escherichia coli*.

The ROS generation is considered a significant indicator of toxic effects in *Artemia salina* (Ates et al., 2013; Wang et al., 2017). Nano-TiO_2 is a well-known photocatalyst that generates ROS under light conditions (Mezni et al., 2018). Cr(VI) is also known to generate ROS intracellularly during the catalytic reduction of Cr(VI) to Cr(III) (Emmanouil et al., 2006; Gu et al., 2015). Thus, both nano-TiO_2 and Cr (VI) could produce ROS intracellularly leading to an additive effect in the mixture groups (Fig. 5). The ROS generated in turn could activate the antioxidant defence mechanisms such as SOD and CAT to protect the cells from oxidative damages. In this regard, SOD activity induced by both the mixture groups were greater compared to that by pristine nano-TiO_2 or Cr(VI) (Fig. 6). This signifies that the mixture containing nano-TiO_2 and Cr(VI) possibly assisted in the activation of SOD. Moreover, the decrease in SOD activity at higher concentrations of the mixture groups might have resulted from the degradation of SOD by the higher amount of ROS in the cells (Gottfredsen et al., 2013). In such instances of reduced enzymatic activity, autocatalysis of oxidative damage follows (Escobar et al., 1996). It is well known that the disproportionation of superoxide produces oxygen and H_2O_2. To overcome the damage produced by H_2O_2 in cells, CAT enzyme is activated. The CAT activity induced by the first mixture group was greater compared to pristine nano-TiO_2 (Fig. 7). This signifies that the enzyme was not denatured even under a remarkably high oxidative stress generated by the mixture group. In contrast, the CAT activity induced by the second mixture group were lesser compared to individual Cr(VI) (Fig. 7). At instances, CAT could not overcome the excess of H_2O_2 produced in the cells and becomes inactivated displaying reduced activity (Zhu et al., 2018).

5. Conclusion and future perspective

The present work studied how a possible interaction of Cr(VI) with nano-TiO_2 might influence their toxic effects on *Artemia salina*. The mortality of *Artemia* salina was mainly dependent on initial uptake of nano-TiO_2 and the adsorption of Cr(VI) to increasing concentrations of nano-TiO_2 resulted in decreased bioavailability of Cr(VI) and reduced toxicity of nano-TiO_2 to *Artemia salina*. In contrast, a strong adsorption of Cr(VI) to nano-TiO_2 and photocatalytic conversion of Cr(VI) to Cr(III) at acidic gut pH, decreased the toxicity of increasing concentrations of Cr(VI) in the presence of fixed concentration of nano-TiO_2.

In the absence of published literature on the co-exposure of nano-TiO_2 and Cr(VI) to *Artemia salina*, the present work would lead to more comprehensive studies in marine ecotoxicology on the interactive effects of the emerging contaminants. Although this study was conducted on the basis of EC_{50} values of nano-TiO_2 and Cr(VI), it is recommended to carry out future studies with environmentally relevant concentrations of the pollutants to look at interactive effects.

CRediT authorship contribution statement

Vignesh Thiagarajan: Investigation, Methodology, Formal analysis, Writing - original draft. **R. Seenivasan:** Conceptualization, Supervision. **David Jenkins:** Writing - review & editing. **N. Chandrasekaran:** Formal analysis, Resources. **Amitava Mukherjee:** Conceptualization, Methodology, Supervision, Project administration, Writing - review & editing.

Declaration of Competing Interest

The authors have no conflicts of interest to declare.

Acknowledgements

The authors are grateful to Vellore Institute of Technology (VIT), Vellore, India for helping them in performing electron microscopic studies.

Appendix A. Supplementary data

Supplementary material related to this article can be found, in the online version, at doi:https://doi.org/10.1016/j.aquatox.2020.105541.

References

Abbott, W.S., 1925. A method of computing the effectiveness of an insecticide. J. Econ. Entomol. 18, 265–267. https://doi.org/10.1093/jee/18.2.265a.

Asuha, S., Zhou, X.G., Zhao, S., 2010. Adsorption of methyl orange and Cr(VI) on mesoporous TiO2 prepared by hydrothermal method. J. Hazard. Mater. 181, 204–210. https://doi.org/10.1016/j.jhazmat.2010.04.117.

Ates, M., Daniels, J., Arslan, Z., Farah, I.O., 2013. Effects of aqueous suspensions of titanium dioxide nanoparticles on Artemia salina: assessment of nanoparticle aggregation, accumulation, and toxicity. Environ. Monit. Assess. 185, 3339–3348. https://doi.org/10.1007/s10661-012-2794-7.

Ates, M., Demir, V., Arslan, Z., Camas, M., Celik, F., 2016. Toxicity of engineered nickel oxide and cobalt oxide nanoparticles to Artemia salina in seawater. Water Air Soil Pollut. 227. https://doi.org/10.1007/s11270-016-2771-9.

Balbi, T., Smerilli, A., Fabbri, R., Ciacci, C., Montagna, M., Grasselli, E., Brunelli, A., Pojana, G., Marcomini, A., Gallo, G., Canesi, L., 2014. Co-exposure to n-TiO2 and Cd2+ results in interactive effects on biomarker responses but not in increased toxicity in the marine bivalve M. galloprovincialis. Sci. Total Environ. 493, 355–364. https://doi.org/10.1016/j.scitotenv.2014.05.146.

Bhuvaneshwari, M., Thiagarajan, V., Nemade, P., Chandrasekaran, N., Mukherjee, A., 2018. Toxicity and trophic transfer of P25 TiO<inf>2</inf>NPs from Dunaliella salina to Artemia salina: effect of dietary and waterborne exposure. Environ. Res. 160. https://doi.org/10.1016/j.envres.2017.09.022.

Bonnand, P., James, R.H., Parkinson, I.J., Connelly, D.P., Fairchild, I.J., 2013. The chromium isotopic composition of seawater and marine carbonates. Earth Planet. Sci. Lett. 382, 10–20. https://doi.org/10.1016/j.epsl.2013.09.001.

Brunelli, A., Pojana, G., Callegaro, S., Marcomini, A., 2013. Agglomeration and sedimentation of titanium dioxide nanoparticles (n-TiO2) in synthetic and real waters. J. Nanopart. Res. 15. https://doi.org/10.1007/s11051-013-1684-4.

Doyle, J.J., Ward, J.E., Mason, R., 2015. An examination of the ingestion, bioaccumulation, and depuration of titanium dioxide nanoparticles by the blue mussel (Mytilus edulis) and the eastern oyster (Crassostrea virginica). Mar. Environ. Res. 110, 45–52. https://doi.org/10.1016/j.marenvres.2015.07.020.

Emmanouil, C., Smart, D.J., Hodges, N.J., Chipman, J.K., 2006. Oxidative damage produced by Cr(VI) and repair in mussel (Mytilus edulis L.) gill. Mar. Environ. Res. 62, S292–S296. https://doi.org/10.1016/j.marenvres.2006.04.024.

Escobar, J.A., Rubio, M.A., Lissi, E.A., 1996. SOD and catalase inactivation by singlet oxygen and peroxyl radicals. Free Radic. Biol. Med. 20, 285–290. https://doi.org/10.1016/0891-5849(95)02037-3.

Fazelian, N., Movafeghi, A., Yousefzadi, M., Rahimzadeh, M., 2019. Cytotoxic impacts of CuO nanoparticles on the marine microalga Nannochloropsis oculata. Environ. Sci. Pollut. Res. 26, 17499–17511. https://doi.org/10.1007/s11356-019-05130-0.

Gottfredsen, R.H., Larsen, U.G., Enghild, J.J., Petersen, S.V., 2013. Hydrogen peroxide induce modifications of human extracellular superoxide dismutase that results in enzyme inhibition. Redox Biol. 1, 24–31. https://doi.org/10.1016/j.redox.2012.12.004.

Gu, Y., Xu, W., Liu, Y., Zeng, G., Huang, J., Tan, X., Jian, H., Hu, X., Li, F., Wang, D., 2015.

Mechanism of Cr(VI) reduction by Aspergillus niger: enzymatic characteristic, oxidative stress response, and reduction product. Environ. Sci. Pollut. Res. 22, 6271–6279. https://doi.org/10.1007/s11356-014-3856-x.
Gupta, G.S., Kansara, K., Shah, H., Rathod, R., Valecha, D., Gogisetty, S., Joshi, P., Kumar, A., 2019. Impact of humic acid on the fate and toxicity of titanium dioxide nanoparticles in Tetrahymena pyriformis and zebrafish embryos. Nanoscale Adv. 1, 219–227. https://doi.org/10.1039/c8na00053k.
Gutner-Hoch, E., Martins, R., Maia, F., Oliveira, T., Shpigel, M., Weis, M., Tedim, J., Benayahu, Y., 2019. Toxicity of engineered micro- and nanomaterials with antifouling properties to the brine shrimp Artemia salina and embryonic stages of the sea urchin Paracentrotus lividus. Environ. Pollut. 251, 530–537. https://doi.org/10.1016/j.envpol.2019.05.031.
Heys, K.A., Shore, R.F., Pereira, M.G., Jones, K.C., Martin, F.L., 2016. Risk assessment of environmental mixture effects. RSC Adv. https://doi.org/10.1039/c6ra05406d.
Hu, S., Han, J., Yang, L., Li, S., Guo, Y., Zhou, B., Wu, H., 2019. Impact of co-exposure to titanium dioxide nanoparticles and Pb on zebrafish embryos. Chemosphere 233, 579–589. https://doi.org/10.1016/j.chemosphere.2019.06.009.
Kono, Y., 1978. Generation of superoxide radical during autoxidation of hydroxylamine and an assay for superoxide dismutase. Arch. Biochem. Biophys. 186, 189–195. https://doi.org/10.1016/0003-9861(78)90479-4.
Kos, M., Kahru, A., Drobne, D., Singh, S., Kalčíková, G., Kühnel, D., Rohit, R., Gotvajn, A.Ž., Jemec, A., 2016. A case study to optimise and validate the brine shrimp Artemia franciscana immobilisation assay with silver nanoparticles: the role of harmonisation. Environ. Pollut. 213, 173–183. https://doi.org/10.1016/j.envpol.2016.02.015.
Li, M., Luo, Z., Yan, Y., Wang, Z., Chi, Q., Yan, C., Xing, B., 2016. Arsenate accumulation, distribution, and toxicity associated with titanium dioxide nanoparticles in Daphnia magna. Environ. Sci. Technol. 50, 9636–9643. https://doi.org/10.1021/acs.est.6b01215.
Li, L., Sillanpää, M., Schultz, E., 2017. Influence of titanium dioxide nanoparticles on cadmium and lead bioaccumulations and toxicities to Daphnia magna. J. Nanopart. Res. 19. https://doi.org/10.1007/s11051-017-3916-5.
Li, M., Pei, J., Tang, X., Guo, X., 2018. Effects of surfactants on the combined toxicity of TiO 2 nanoparticles and cadmium to Escherichia coli. J. Environ. Sci. (China). https://doi.org/10.1016/j.jes.2018.02.016.
Lu, J., Zhu, X., Tian, S., Lv, X., Chen, Z., Jiang, Y., Liao, X., Cai, Z., Chen, B., 2018. Graphene oxide in the marine environment: toxicity to Artemia salina with and without the presence of Phe and Cd 2+. Chemosphere 211, 390–396. https://doi.org/10.1016/j.chemosphere.2018.07.140.
Luo, Z., Wang, Z., Yan, Y., Li, J., Yan, C., Xing, B., 2018. Methods of determining titanium dioxide nanoparticles enhance inorganic arsenic bioavailability and methylation in two freshwater algae species. MethodsX 5, 620–625. https://doi.org/10.1016/j.mex.2018.06.004.
Manzo, S., Buono, S., Rametta, G., Miglietta, M., Schiavo, S., Di Francia, G., 2015. The diverse toxic effect of SiO2 and TiO2 nanoparticles toward the marine microalgae Dunaliella tertiolecta. Environ. Sci. Pollut. Res. 22, 15941–15951. https://doi.org/10.1007/s11356-015-4790-2.
Marinho, B.A., Cristóvão, R.O., Djellabi, R., Loureiro, J.M., Boaventura, R.A.R., Vilar, V.J.P., 2017. Photocatalytic reduction of Cr(VI) over TiO2-coated cellulose acetate monolithic structures using solar light. Appl. Catal. B Environ. 203, 18–30. https://doi.org/10.1016/j.apcatb.2016.09.061.
Matouke, M.M., Mustapha, M.K., 2019. Antagonistic effects of binary mixture of titanium dioxide nanoparticles and lead on biomass and oxidative stress in exposed Chloroidium ellipsoideum (Gerneck). Polish J. Nat. Sci. 34, 367–382.
Mezni, A., Alghool, S., Sellami, B., Ben Saber, N., Altalhi, T., 2018. Titanium dioxide nanoparticles: synthesis, characterisations and aquatic ecotoxicity effects. Chem. Ecol. 34, 288–299. https://doi.org/10.1080/02757540.2017.1420178.
Oze, C., Bird, D.K., Fendorf, S., 2007. Genesis of hexavalent chromium from natural sources in soil and groundwater. Proc. Natl. Acad. Sci. U. S. A. 104, 6544–6549. https://doi.org/10.1073/pnas.0701085104.
Ozkan, Y., Altinok, I., Ilhan, H., Sokmen, M., 2016. Determination of TiO 2 and AgTiO 2 Nanoparticles in Artemia salina: toxicity, morphological changes, uptake and depuration. Bull. Environ. Contam. Toxicol. 96, 36–42. https://doi.org/10.1007/s00128-015-1634-1.
Pađan, J., Marcinek, S., Cindrić, A.-M., Layglon, N., Lenoble, V., Salaün, P., Garnier, C., Omanović, D., 2019. Improved voltammetric methodology for chromium redox speciation in estuarine waters. Anal. Chim. Acta. https://doi.org/10.1016/j.aca.2019.09.014.
Parmar, T.K., Rawtani, D., Agrawal, Y.K., 2016. Bioindicators: the natural indicator of environmental pollution. Front. Life Sci. 9, 110–118. https://doi.org/10.1080/21553769.2016.1162753.
Persoone, G., Van de Vel, A., Van Steertegem, M., De Nayer, B., 1989. Predictive value of laboratory tests with aquatic invertebrates: influence of experimental conditions. Aquat. Toxicol. 14, 149–167. https://doi.org/10.1016/0166-445X(89)90025-8.
Schiavo, S., Oliviero, M., Li, J., Manzo, S., 2018. Testing ZnO nanoparticle ecotoxicity: linking time variable exposure to effects on different marine model organisms. Environ. Sci. Pollut. Res. 25, 4871–4880. https://doi.org/10.1007/s11356-017-0815-3.
Sharma, P., Bihari, V., Agarwal, S.K., Verma, V., Kesavachandran, C.N., Pangtey, B.S., Mathur, N., Singh, K.P., Srivastava, M., Goel, S.K., 2012. Groundwater contaminated with hexavalent chromium [Cr (VI)]: a health survey and clinical examination of community inhabitants (Kanpur, India). PLoS One 7. https://doi.org/10.1371/journal.pone.0047877.
Tchounwou, P.B., Yedjou, C.G., Patlolla, A.K., Sutton, D.J., 2012. Heavy metal toxicity and the environment. EXS. https://doi.org/10.1007/978-3-7643-8340-4_6.
Thiagarajan, V., Natarajan, L., Seenivasan, R., Chandrasekaran, N., Mukherjee, A., 2019. Tetracycline affects the toxicity of P25 n-TiO2 towards marine microalgae Chlorella sp. Environ. Res., 108808. https://doi.org/10.1016/j.envres.2019.108808.
Vimercati, L., Gatti, M.F., Gagliardi, T., Cuccaro, F., De Maria, L., Caputi, A., Quarato, M., Baldassarre, A., 2017. Environmental exposure to arsenic and chromium in an industrial area. Environ. Sci. Pollut. Res. 24, 11528–11535. https://doi.org/10.1007/s11356-017-8827-6.
Wang, H., Joseph, J.A., 1999. Quantifying cellular oxidative stress by dichlorofluorescein assay using microplate reader. Free Radic. Biol. Med. 27, 612–616. https://doi.org/10.1016/S0891-5849(99)00107-0.
Wang, X., Pehkonen, S.O., Ray, A.K., 2004. Removal of Aqueous Cr(VI) by a combination of photocatalytic reduction and coprecipitation. Ind. Eng. Chem. Res. 43, 1665–1672. https://doi.org/10.1021/ie030580j.
Wang, C., Jia, H., Zhu, L., Zhang, H., Wang, Y., 2017. Toxicity of α-Fe2O3 nanoparticles to Artemia salina cysts and three stages of larvae. Sci. Total Environ. 598, 847–855. https://doi.org/10.1016/j.scitotenv.2017.04.183.
Weng, C.H., Wang, J.H., Huang, C.P., 1997. Adsorption of Cr(VI) onto TiO2 from dilute aqueous solutions. Water Sci. Technol. 35, 55–62. https://doi.org/10.1016/S0273-1223(97)00114-5.
Yang, J.K., Lee, S.M., 2006. Removal of Cr(VI) and humic acid by using TiO2 photocatalysis. Chemosphere 63, 1677–1684. https://doi.org/10.1016/j.chemosphere.2005.10.005.
Yilancioglu, K., Cokol, M., Pastirmaci, I., Erman, B., Cetiner, S., 2014. Oxidative stress is a mediator for increased lipid accumulation in a newly isolated Dunaliella salina strain. PLoS One 9. https://doi.org/10.1371/journal.pone.0091957.
Zhu, B., Zhu, S., Li, J., Hui, X., Wang, G.X., 2018. The developmental toxicity, bioaccumulation and distribution of oxidized single walled carbon nanotubes in: Artemia salina. Toxicol. Res. (Camb). 7, 897–906. https://doi.org/10.1039/c8tx00084k.